Bo Hu[1]
e-mail: hubo@ysu.edu.cn

Jingjing Yu
e-mail: yujingjing_725@126.com

Yi Lu
e-mail: luyi@ysu.edu.cn

Robotics Research Center,
Yanshan University,
Qinhuangdao,
Hebei 066004, P. R. China

Chunping Sui
e-mail: cpsui@sia.cn

Jianda Han
e-mail: jdhan@sia.cn

State Key Laboratory of Robotics,
Shenyang Institute of Automation,
Chinese Academy of Sciences,
Shenyang, Liaoning 110016, P. R. China

Statics and Stiffness Model of Serial-Parallel Manipulator Formed by *k* Parallel Manipulators Connected in Series

The statics and stiffness model of serial-parallel manipulators (S-PMs) formed by k *parallel manipulators (PMs) connected in series is established in this paper. The S-PMs can provide features of both serial manipulators (SMs) and PMs. First, the unified formulae for solving the statics and stiffness of S-PMs are derived. Second, a k(PS + RPS + SPS) S-PM is analyzed to illustrate this model. Finally, an analytic solved example for 5(PS + RPS + SPS) S-PM is given. The established model can offer an essential theoretical basis for S-PMs.* [DOI: 10.1115/1.4006190]

Keywords: serial-parallel manipulator, kinematics, statics, stiffness

1 Introduction

Both SMs and PMs have their merits in robot manipulators. The PMs have some merits such as higher stiffness, higher precision, good stability, and easier control. Recently, the theory and application research for various novel limited-dof PMs have became a very important research direction and a front technology [1,2]. Some subjects, such as kinematics, singularity, stiffness, dynamics, etc. [3–9], have been widely studied.

The S-PMs have the advantages of both SMs and PMs from rigidity and workspace [10–18]. The fundamental theory of single PMs has been going maturity. However, the S-PMs have not been investigated deeply. In this aspect, Romdhane [10] designed and analyzed a hybrid S-PM formed by a pure translational and a pure rotational PMs, which have passive legs. Tanev [11] solved the forward and inverse position problems of a hybrid manipulator. Zheng et al. [12] studied the kinematics of a hybrid S-PM formed by a pure translational and a pure rotational 3-universal jointprismatic pair-universal joint (UPU) PM by using quaternion. Lu and Hu [13] solved driving forces of 2(3-spherical joint-prismatic joint-revolute joint (SPR)) S-PM by Computer Aided Design (CAD) variation geometry approach and solved the velocity, acceleration, statics, and stiffness, subsequently [14,15]. Gallardoa et al. [16,17] studied the kinematics and dynamic of S-PM via screw theory and principle of virtual work. Ibrahim and Khalil [18] established inverse and direct dynamic models of hybrid robots by means of the recursive Newton–Euler algorithms.

The previous research for such manipulators mainly focused on the S-PM formed by 2 PMs, the S-PMs formed by any number of PMs connected in series have been seldom studied due to their complicated structure. In order to obtain larger workspace, high flexibility and avoid obstacles and singularities, the *k* S-PMs are more applicable than 2 S-PMs. These type manipulators can be used as spatial truss, biomimetic snake, elephant's trunk, biosimulation manipulator, and so on [19–22].

The systemic theory for S-PMs formed by any number of PMs has not been established. This paper focuses on establishing systemic kinematics, statics and stiffness model of S-PMs. Due to the complicated structure, the force transmission regularities of such manipulators have not been systematically revealed. Stiffness is one of the important indexes for evaluating performances of S-PM, particularly when the S-PMs are used as robot arm and machine tools. High stiffness allows higher machining speed with high accuracy of the terminal effector. The statics and stiffness model for S-PM is more complex than SMs and PMs. Up to now, there is not a unified model for these problems. It is a significant and challenging issue to establish the statics and stiffness model for S-PM.

2 Kinematics of S-PM Formed by *k* PMs Connected in Series

Suppose one S-PM is formed by *k* PMs connected in series. Let the *k* PMs named PM 1, PM 2, …, PM *k* in sequence from bottom to up. The upper platform of PM *i*-1 ($i = 2, \ldots, k$) and the base of PM *i* are fixed with their centers kept coincidence. Let o_i denotes the center of the upper platform of PM *i*.

Establishing coordinate frames $\{n_{i0}\}$ and $\{n_{i1}\}$ at the center of the lower platform and upper platform of PM *i*, respectively. Then, $\{n_{10}\}$ can be seen as the base coordinate frame and $\{n_{k1}\}$ can be seen as the terminal coordinate frame.

The center of the terminal platform ${}^{n_{10}}\boldsymbol{o}_k$ can be expressed as follows:

$$
\begin{aligned}
&{}^{n_{10}}\boldsymbol{o}_k = \sum_{i=1}^{k} {}^{n_{10}}_{n_{i0}}\mathbf{R}\,{}^{n_{i0}}\boldsymbol{o}_i,\\
&{}^{n_{10}}_{n_{i0}}\mathbf{R} = {}^{n_{10}}_{n_{10}}\mathbf{R}\left({}^{n_{10}}_{n_{11}}\mathbf{R}\,{}^{n_{11}}_{n_{20}}\mathbf{R}\right)\cdots\left({}^{n_{(i-1)0}}_{n_{(i-1)1}}\mathbf{R}\,{}^{(i-1)1}_{n_{i0}}\mathbf{R}\right),\\
&{}^{n_{10}}_{n_{10}}\mathbf{R} = \mathbf{E}_{3\times3}, \mathbf{E}_{3\times3} = \begin{bmatrix} 1 & 0 & 0\\ 0 & 1 & 0\\ 0 & 0 & 1 \end{bmatrix}
\end{aligned}
\tag{1}
$$

[1]Corresponding author.

Contributed by the Mechanisms and Robotics Committee of ASME for publication in the Journal of Mechanisms and Robotics. Manuscript received December 30, 2010; final manuscript received January 9, 2012; published online April 25, 2012. Assoc. Editor: Federico Thomas.

A composite rotational matrix ${}^{n_{10}}_{n_{k1}}\mathbf{R}$ from $\{n_{k1}\}$ to $\{n_{10}\}$ can be expressed as follows:

$$ {}^{n_{10}}_{n_{k1}}\mathbf{R} = \left({}^{n_{10}}_{n_{10}}\mathbf{R}{}^{n_{10}}_{n_{11}}\mathbf{R}\right)\left({}^{n_{11}}_{n_{20}}\mathbf{R}{}^{n_{20}}_{n_{21}}\mathbf{R}\right)\cdots\left({}^{n_{(i-1)1}}_{n_{i0}}\mathbf{R}{}^{n_{i0}}_{n_{i1}}\mathbf{R}\right)\cdots\left({}^{n_{(k-1)1}}_{n_{k0}}\mathbf{R}{}^{k0}_{n_{k1}}\mathbf{R}\right) \tag{2} $$

The angular velocity of the terminal platform relative to n_o can be derived as

$$ \begin{aligned} {}^{n_{10}}_{n_{k1}}\boldsymbol{\omega} &= \sum_{i=1}^{k} {}^{n_{10}}_{n_{i0}}\mathbf{R}{}^{n_{i0}}_{n_{i1}}\boldsymbol{\omega}, \\ {}^{n_{10}}_{n_{i1}}\mathbf{R} &= {}^{n_{10}}_{n_{i0}}\mathbf{R}{}^{n_{i0}}_{n_{i1}}\mathbf{R},\ {}^{n_{10}}_{n_{i1}}\mathbf{R} = {}^{n_{10}}_{n_{11}}\mathbf{R}\left({}^{n_{11}}_{n_{20}}\mathbf{R}{}^{n_{20}}_{n_{21}}\mathbf{R}\right)\cdots\left({}^{n_{(i-1)1}}_{n_{i0}}\mathbf{R}{}^{n_{i0}}_{n_{i1}}\mathbf{R}\right) \end{aligned} \tag{3} $$

Differentiating both sides of Eq. (1) with respect to time, ${}^{n_{10}}\boldsymbol{v}_{ok}$ can be expressed as follows:

$$ {}^{n_{10}}\boldsymbol{v}_{ok} = \sum_{i=1}^{k}\left[{}^{n_{10}}_{n_{i0}}\mathbf{R}{}^{n_{i0}}\boldsymbol{v}_{oi} + \left({}^{n_{10}}_{n_{i0}}\boldsymbol{\omega}\times{}^{n_{10}}_{n_{i0}}\mathbf{R}\right){}^{n_{i0}}\boldsymbol{o}_i\right] \tag{4} $$

Differentiating both sides of Eq. (3) with respect to time, ${}^{n_0}_{n_k}\boldsymbol{\varepsilon}$ can be expressed as follows:

$$ {}^{n_{10}}_{n_{k1}}\boldsymbol{\varepsilon} = \sum_{i=1}^{k}\left[{}^{n_{10}}_{n_{i0}}\mathbf{R}{}^{n_{i0}}_{n_{i1}}\boldsymbol{\varepsilon} + \left({}^{n_{10}}_{n_{i0}}\boldsymbol{\omega}\times{}^{n_{10}}_{n_{i0}}\mathbf{R}\right){}^{n_{i0}}_{n_{i1}}\boldsymbol{\omega}\right] \tag{5} $$

Let $\boldsymbol{t} = [t_x\ t_y\ t_z]^T$, $\boldsymbol{s} = [s_x\ s_y\ s_z]^T$ be two arbitrary vectors, $\mathbf{S}(t)$ be a skew-symmetric matrix. There must be

$$ \mathbf{S}(t) = \begin{bmatrix} 0 & -t_z & t_y \\ t_z & 0 & -t_x \\ -t_y & t_x & 0 \end{bmatrix},\quad \mathbf{S}(t) = -\mathbf{S}(t)^T,\quad \boldsymbol{t}\times\boldsymbol{s} = \mathbf{S}(t)\boldsymbol{s} \tag{6} $$

Differentiating both sides of Eq. (4) with respect to time and combining with Eq. (6), ${}^{n_{10}}\boldsymbol{a}_{ok}$ can be expressed as follows:

$$ \begin{aligned} {}^{n_{10}}\boldsymbol{a}_{ok} &= \sum_{i=1}^{k}\left\{\begin{array}{l} {}^{n_{10}}_{n_{i0}}\mathbf{R}{}^{n_{i0}}\boldsymbol{a}_{oi} + 2\left({}^{n_{10}}_{n_{i0}}\boldsymbol{\omega}\times{}^{n_{10}}_{n_{i0}}\mathbf{R}\right)\cdot{}^{n_{i0}}\boldsymbol{v}_{oi} \\ +\left[{}^{n_{10}}_{n_{i0}}\boldsymbol{\varepsilon}\times{}^{n_{10}}_{n_{i0}}\mathbf{R} + {}^{n_{10}}_{n_{i0}}\boldsymbol{\omega}\times\left({}^{n_{10}}_{n_{i0}}\boldsymbol{\omega}\times{}^{n_{10}}_{n_{i0}}\mathbf{R}\right)\right]\cdot{}^{n_{i0}}\boldsymbol{o}_i \end{array}\right\} \\ &= \sum_{i=1}^{k}\left\{\begin{array}{l} {}^{n_{10}}_{n_{i0}}\mathbf{R}{}^{n_{i0}}\boldsymbol{a}_{oi} - 2S\left({}^{n_{10}}_{n_{i0}}\mathbf{R}{}^{n_{i0}}\boldsymbol{v}_{oi}\right)\cdot{}^{n_{10}}_{n_{i0}}\boldsymbol{\omega} \\ -S\left({}^{n_{10}}_{n_{i0}}\mathbf{R}{}^{n_{i0}}\boldsymbol{o}_i\right){}^{n_{10}}_{n_{i0}}\boldsymbol{\varepsilon} + S\left({}^{n_{10}}_{n_{i0}}\boldsymbol{\omega}\right)^2{}^{n_{10}}_{n_{i0}}\mathbf{R}{}^{n_{i0}}\boldsymbol{o}_i \end{array}\right\} \end{aligned} \tag{7} $$

${}^{n_{i0}}\boldsymbol{o}_i$, ${}^{n_{i0}}\boldsymbol{v}_{oi}$, ${}^{n_{i0}}_{n_{i1}}\boldsymbol{\omega}$, ${}^{n_{i0}}_{n_{i1}}\boldsymbol{\varepsilon}$, and ${}^{n_{i0}}\boldsymbol{a}_{oi}$ can be solved in PM i when given the corresponding acceleration, velocity, and position of actuators.

3 Statics and Stiffness of S-PM Formed by k PMs Connected in Series

From Eq. (4) leads to

$$ \begin{aligned} {}^{n_{10}}\boldsymbol{v}_{ok} &= \sum_{i=1}^{k}{}^{n_{10}}_{n_{i0}}\mathbf{R}{}^{n_{i0}}\boldsymbol{v}_{oi} \\ &- \sum_{i=1}^{k-1}\left\{\left[\sum_{j=i}^{k-1}S\left({}^{n_{10}}_{n_{(j+1)0}}\mathbf{R}{}^{n_{(j+1)0}}\boldsymbol{o}_{j+1}\right)\right]{}^{n_{10}}_{n_{i0}}\mathbf{R}{}^{n_{i0}}_{n_{i1}}\boldsymbol{\omega}\right\}(k\geq 2) \end{aligned} \tag{8a} $$

By combining Eq. (3) with Eq. (8a), the terminal velocity can be expressed as follows:

$$ \begin{aligned} &\begin{bmatrix} {}^{n_{10}}\boldsymbol{v}_{ok} \\ {}^{n_{10}}_{n_{k1}}\boldsymbol{\omega} \end{bmatrix} = \sum_{i=1}^{k}\mathbf{J}_{Ri}\begin{bmatrix} {}^{n_{i0}}\boldsymbol{v}_{oi} \\ {}^{n_{i0}}_{n_{i1}}\boldsymbol{\omega} \end{bmatrix}(k\geq 2), \\ &\mathbf{J}_{Ri} = \begin{bmatrix} {}^{n_{10}}_{n_{i0}}\mathbf{R} & -\left[\sum_{j=i}^{k-1}S\left({}^{n_{10}}_{n_{(j+1)0}}\mathbf{R}{}^{n_{(j+1)0}}\boldsymbol{o}_{j+1}\right)\right]{}^{n_{10}}_{n_{i0}}\mathbf{R} \\ \mathbf{0}_{3\times3} & {}^{n_{10}}_{n_{i0}}\mathbf{R} \end{bmatrix}(i<k), \\ &\mathbf{J}_{Rk} = \begin{bmatrix} {}^{n_{10}}_{n_{i0}}\mathbf{R} & \mathbf{0}_{3\times3} \\ \mathbf{0}_{3\times3} & {}^{n_{10}}_{n_{i0}}\mathbf{R} \end{bmatrix}(i=k) \end{aligned} \tag{8b} $$

From Eq. (8b) and the principle of virtual work lead to

$$ \begin{aligned} \boldsymbol{F}_{s1}^{\mathrm{T}}\boldsymbol{v}_{s1} + \boldsymbol{F}_{s2}^{\mathrm{T}}\boldsymbol{v}_{s2} + \cdots + \boldsymbol{F}_{sk}^{\mathrm{T}}\boldsymbol{v}_{sk} &= -\begin{bmatrix} {}^{n_0}\boldsymbol{F}_o \\ {}^{n_0}\boldsymbol{T}_o \end{bmatrix}^{\mathrm{T}}\begin{bmatrix} {}^{n_0}\boldsymbol{v}_{ok} \\ {}^{n_0}_{n_k}\boldsymbol{\omega} \end{bmatrix} \\ &= -\begin{bmatrix} {}^{n_0}\boldsymbol{F}_o \\ {}^{n_0}\boldsymbol{T}_o \end{bmatrix}^{\mathrm{T}}\sum_{i=1}^{k}\mathbf{J}_{Ri}\begin{bmatrix} {}^{n_{i0}}\boldsymbol{v}_{oi} \\ {}^{n_{i0}}_{n_{i1}}\boldsymbol{\omega} \end{bmatrix} \\ &= -\begin{bmatrix} {}^{n_0}\boldsymbol{F}_o \\ {}^{n_0}\boldsymbol{T}_o \end{bmatrix}^{\mathrm{T}}\sum_{i=1}^{k}\mathbf{J}_{Ri}\mathbf{J}_{si}^{-1}\boldsymbol{v}_{si} \end{aligned} \tag{9} $$

From Eq. (9) leads to

$$ \begin{bmatrix} \boldsymbol{F}_{s1}^{\mathrm{T}} & \cdots & \boldsymbol{F}_{sk}^{\mathrm{T}} \end{bmatrix}\begin{bmatrix} \boldsymbol{V}_{s1} \\ \vdots \\ \boldsymbol{V}_{sk} \end{bmatrix} = -\begin{bmatrix} {}^{n_0}\boldsymbol{F}_o \\ {}^{n_0}\boldsymbol{T}_o \end{bmatrix}^{\mathrm{T}}\begin{bmatrix} \mathbf{J}_{R1}\mathbf{J}_{s1}^{-1} & \cdots & \mathbf{J}_{Rk}\mathbf{J}_{sk}^{-1} \end{bmatrix}\begin{bmatrix} \boldsymbol{V}_{s1} \\ \vdots \\ \boldsymbol{V}_{sk} \end{bmatrix} \tag{10} $$

From Eq. (10) leads to

$$ \boldsymbol{F}_{si} = -\left(\mathbf{J}_{Ri}\mathbf{J}_{si}^{-1}\right)^{\mathrm{T}}\begin{bmatrix} {}^{n_0}\boldsymbol{F}_o \\ {}^{n_0}\boldsymbol{T}_o \end{bmatrix} \tag{11} $$

The statics of PM i can be solved from Eq. (11).

For single PM i, the following formulae are satisfied

$$ \delta\boldsymbol{\rho}_i = \mathbf{K}_i^{-1}\begin{bmatrix} {}^{n_i}\boldsymbol{F}_{oi} \\ {}^{n_i}\boldsymbol{T}_{oi} \end{bmatrix},\ \begin{bmatrix} {}^{n_i}\boldsymbol{F}_{oi} \\ {}^{n_i}\boldsymbol{T}_{oi} \end{bmatrix} = -\mathbf{J}_{si}^{\mathrm{T}}\boldsymbol{F}_{si} \tag{12} $$

From Eqs. (11) and (12) lead to

$$ \begin{bmatrix} {}^{n_i}\boldsymbol{F}_{oi} \\ {}^{n_i}\boldsymbol{T}_{oi} \end{bmatrix} = \mathbf{J}_{Ri}^{\mathrm{T}}\begin{bmatrix} {}^{n_0}\boldsymbol{F}_o \\ {}^{n_0}\boldsymbol{T}_o \end{bmatrix} \tag{13} $$

From Eqs. (8b), (12), and (13) lead to

$$ \delta\boldsymbol{\rho} = \sum_{i=1}^{k}\mathbf{J}_{Ri}\delta\boldsymbol{\rho}_i = \sum_{i=1}^{k}\left(\mathbf{J}_{Ri}\mathbf{K}_i^{-1}\mathbf{J}_{Ri}^{\mathrm{T}}\right)\begin{bmatrix} {}^{n_0}\boldsymbol{F}_o \\ {}^{n_0}\boldsymbol{T}_o \end{bmatrix} \tag{14} $$

From Eq. (14) leads to

$$ \begin{bmatrix} {}^{n_0}\boldsymbol{F}_o \\ {}^{n_0}\boldsymbol{T}_o \end{bmatrix} = \mathbf{K}\delta\boldsymbol{\rho},\quad \mathbf{K} = \left(\sum_{i=1}^{k}\mathbf{J}_{Ri}\mathbf{K}_i^{-1}\mathbf{J}_{Ri}^{\mathrm{T}}\right)^{-1} \tag{15} $$

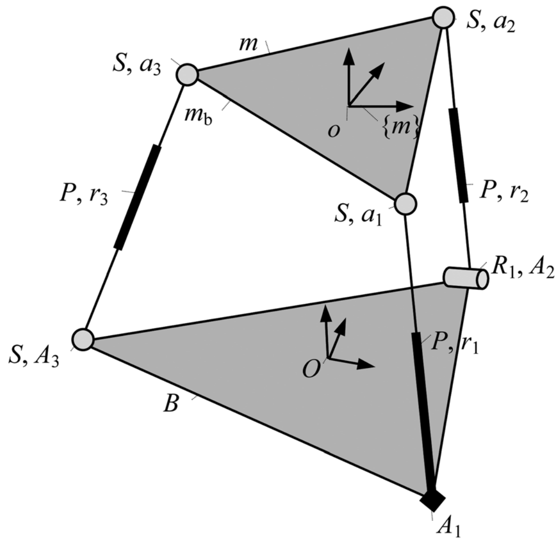

Fig. 1 Sketch of PS + RPS + SPS PM

Equation (15) is the stiffness matrix of a S-PM formed by k PMs connected in series.

4 Statics and Stiffness of a k(PS + RPS + SPS) PM

In this section, the k(PS + RPS + SPS) PM formed by k PS + RPS + SPS PMs is analyzed to illustrate the model (see Fig. 1).

4.1 Analysis of PS + RPS + SPS PM. The PS + RPS + SPS PM includes a moving platform m, a base B, and three different type active legs r_1, r_2, and r_3. Here, m is a regular triangle with o as its center and three vertices a_i ($i = 1, 2, 3$), B is a regular triangle with O as its center and three vertices A_i ($i = 1, 2, 3$). The first active limb r_1 is a PS-type limb, this limb connects m with B by using a spherical joint S at a_1 on m, a prismatic joint P, and be perpendicularly fixed at A_1 on B. The second active limb r_2 is a RPS-type limb, r_2 connects m with B by using a spherical joint S at a_2 on m, a prismatic joint P along r_2, and a revolute joint R_1 at A_2 on B. The revolute joint is lying in B and perpendicular to A_1A_2. The third active limb r_3 is a SPS-type limb, this limb connects m with B by using a spherical joint S at a_3 on m, a prismatic joint P along r_3, and a spherical joint S at A_3 on B.

Let $\perp$ be a perpendicular constraint and $\|$ be a parallel constraint, respectively. Then, there must be some geometrical constraint as follows:

$$r_1 \perp B, r_2 \perp R_1, R_1 \perp A_1A_2 \tag{16}$$

4.1.1 Inverse and Forward Position Analysis of PS + RPS + SPS PM. Let $\{B\}$ be a frame O-XYZ attached on B at O, $\{m\}$ be a frame o-xyz attached on m at o. Some geometrical conditions ($x \perp a_1a_2$, $y \| a_1a_2$, $z \perp m$, $X \perp A_1A_2$, $Y \| A_1A_2$, $Z \perp B$) are satisfied.

The coordinate A_i ($i = 1, 2, 3$) and o in $\{B\}$ can be expressed as follows:

$$\boldsymbol{A}_1 = \begin{bmatrix} X_{A1} \\ Y_{A1} \\ Z_{A1} \end{bmatrix} = \frac{1}{2}\begin{bmatrix} L \\ -qL \\ 0 \end{bmatrix}, \quad \boldsymbol{A}_2 = \begin{bmatrix} X_{A2} \\ Y_{A2} \\ Z_{A2} \end{bmatrix} = \frac{1}{2}\begin{bmatrix} L \\ qL \\ 0 \end{bmatrix},$$

$$\boldsymbol{A}_3 = \begin{bmatrix} X_{A3} \\ Y_{A3} \\ Z_{A3} \end{bmatrix} = \begin{bmatrix} -L \\ 0 \\ 0 \end{bmatrix}, \quad \boldsymbol{o} = \begin{bmatrix} X_o \\ Y_o \\ Z_o \end{bmatrix} \tag{17a}$$

The point a_i ($i = 1, 2, 3$) in $\{m\}$ can be expressed as follows:

$${}^m\boldsymbol{a}_1 = \begin{bmatrix} x_{a1} \\ y_{a1} \\ z_{a1} \end{bmatrix} = \frac{1}{2}\begin{bmatrix} l \\ -ql \\ 0 \end{bmatrix}, {}^m\boldsymbol{a}_2 = \begin{bmatrix} x_{a2} \\ y_{a2} \\ z_{a2} \end{bmatrix} = \frac{1}{2}\begin{bmatrix} l \\ ql \\ 0 \end{bmatrix},$$

$${}^m\boldsymbol{a}_3 = \begin{bmatrix} x_{a3} \\ y_{a3} \\ z_{a3} \end{bmatrix} = \begin{bmatrix} -l \\ 0 \\ 0 \end{bmatrix} \tag{17b}$$

where L is the distance from O to A_i, l is the distance from o to a_i, and q is a constant with $q = 3^{1/2}$.

a_i ($i = 1, 2, 3$) and o in $\{B\}$ can be expressed as follows:

$$\boldsymbol{a}_1 = \frac{1}{2}\begin{bmatrix} lx_l - qly_l + 2X_o \\ lx_m - qly_m + 2Y_o \\ lx_n - qly_n + 2Z_o \end{bmatrix}, \quad \boldsymbol{a}_2 = \frac{1}{2}\begin{bmatrix} lx_l + qly_l + 2X_o \\ lx_m + qly_m + 2Y_o \\ lx_n + qly_n + 2Z_o \end{bmatrix},$$

$$\boldsymbol{a}_3 = \begin{bmatrix} -lx_l + X_o \\ -lx_m + Y_o \\ -lx_n + Z_o \end{bmatrix} \tag{17c}$$

here, $\boldsymbol{o}$ is the position of the center of m and ${}^B_m\mathbf{R}$ is the rotational transformation matrix from $\{m\}$ to $\{B\}$. (x_l, x_m, x_n, y_l, y_m, y_n, z_l, z_m, z_n) are nine orientation parameters of m, their constrained equations can be derived in Refs. [1,2].

The geometric constraint for PS + SPR + SPS parallel manipulator can be written as follows:

$$\boldsymbol{A}_1\boldsymbol{a}_1 \perp \boldsymbol{X}, \quad \boldsymbol{A}_1\boldsymbol{a}_1 \perp \boldsymbol{Y}, \quad \boldsymbol{A}_2\boldsymbol{a}_2 \perp \boldsymbol{X} \tag{18a}$$

$$\boldsymbol{A}_1\boldsymbol{a}_1 \cdot \boldsymbol{X} = 0, \quad \boldsymbol{A}_1\boldsymbol{a}_1 \cdot \boldsymbol{Y} = 0, \quad \boldsymbol{A}_2\boldsymbol{a}_2 \cdot \boldsymbol{X} = 0 \tag{18b}$$

The constraint equations are derived from constrained equations of (x_l, x_m, x_n, y_l, y_m, y_n, z_l, z_m, z_n) and Eq. (18b) as follows:

$$\begin{aligned} ex_l - qly_l + 2X_o - L &= 0 \\ ex_m - qly_m + 2Y_o + qL &= 0 \\ ex_l + qly_l + 2X_o - L &= 0 \end{aligned} \tag{19}$$

From Eqs. (19), the following equations can be derived:

$$y_l = 0, \quad X_o = \frac{L - lx_l}{2}, \quad Y_o = \frac{qly_m - lx_m - qL}{2} \tag{20}$$

Let three Euler angles α, β, and λ rotate about the x-, z-, and y-axis of the moved reference frame. Thus, the rotational transformation matrix can be expressed as follows:

$${}^B_m\mathbf{R} = \begin{bmatrix} c_\beta c_\lambda & -s_\beta & c_\beta s_\lambda \\ c_\alpha s_\beta c_\lambda + s_\alpha s_\lambda & c_\alpha c_\beta & c_\alpha s_\beta s_\lambda - s_\alpha c_\lambda \\ s_\alpha s_\beta c_\lambda - c_\alpha s_\lambda & s_\alpha c_\beta & s_\alpha s_\beta s_\lambda + c_\alpha c_\lambda \end{bmatrix} \tag{21}$$

From Eqs. (20) and (21) lead to

$$\beta = 0 \tag{22}$$

Then, the rotational transformation matrix can be predigested as follows:

$$
{}^{B}_{m}\mathbf{R} = \begin{bmatrix} c_\lambda & 0 & s_\lambda \\ s_\alpha s_\lambda & c_\alpha & -s_\alpha c_\lambda \\ -c_\alpha s_\lambda & s_\alpha & c_\alpha c_\lambda \end{bmatrix} \tag{23}
$$

From Eqs. (20) and (23) lead to

$$
\begin{aligned}
X_o &= \frac{L - l x_l}{2} = \frac{L - l c_\lambda}{2} \\
Y_o &= \frac{q l y_m - l x_m - qL}{2} = \frac{q l c_\alpha - l s_\alpha s_\lambda - qL}{2}
\end{aligned} \tag{24}
$$

The inverse kinematics can be derived as follows:

$$
r_i^2 = |\boldsymbol{a}_i - \boldsymbol{A}_i|^2 \quad (i = 1, 2, 3) \tag{25}
$$

Equation (25) can be expanded as follows:

$$
\begin{aligned}
r_1^2 &= l^2 + L^2 + (X_o^2 + Y_o^2 + Z_o^2) + l(X_o x_l + Y_o x_m + Z_o x_n) \\
&\quad - L l x_l/2 + qLl x_m/2 - ql(X_o y_l + Y_o y_m + Z_o y_n) \\
&\quad + qLl(y_l - q y_m)/2 - L(X_o - qY_o)
\end{aligned} \tag{26a}
$$

$$
\begin{aligned}
r_2^2 &= l^2 + L^2 + (X_o^2 + Y_o^2 + Z_o^2) + l(X_o x_l + Y_o x_m + Z_o x_n) \\
&\quad - L l x_l/2 - qLl x_m/2 + ql(X_o y_l + Y_o y_m + Z_o y_n \\
&\quad - qLl(y_l + q y_m)/2 - L(X_o + qY_o)
\end{aligned} \tag{26b}
$$

$$
\begin{aligned}
r_3^2 &= X_o^2 + Y_o^2 + Z_o^2 + L^2 + l^2 - 2l(X_o x_l + Y_o x_m + Z_o x_n) \\
&\quad + 2L(-l x_l + X_o)
\end{aligned} \tag{26c}
$$

When given the independent parameters (α, λ, Z_o), X_o, Y_o and the items of ${}^{B}_{m}\mathbf{R}$ can be expressed by the three independent parameters α, λ, and Z_o. Then, from Eqs. (26a) to (26c), r_i ($i = 1, 2, 3$) can be derived.

As $r_1 \perp B$ leads to

$$
r_1 \begin{bmatrix} 0 \\ 0 \\ 1 \end{bmatrix} = \boldsymbol{a}_1 - \boldsymbol{A}_1 = \frac{1}{2} \begin{bmatrix} l c_\lambda + 2X_o - L \\ l s_\alpha s_\lambda - q l c_\alpha + 2Y_o + qL \\ -l c_\alpha s_\lambda - q l s_\alpha + 2Z_o \end{bmatrix} \tag{27}
$$

From Eq. (27) leads to

$$
Z_o = \frac{2r_1 - l x_n + q l y_n}{2} = \frac{2r_1 + l c_\alpha s_\lambda + q l s_\alpha}{2} \tag{28}
$$

From Eqs. (24), (28), and (26a)–(26c) lead to

$$
r_2^2 - r_1^2 = 3(L^2 + l^2) + 2q l r_1 s_\alpha - 6Ll c_\alpha \tag{29}
$$

$$
\begin{aligned}
r_2^2 + r_1^2 - 2r_3^2 &= -3l(2r_1 c_\alpha + qL s_\alpha) s_\lambda \\
&\quad - 3Ll c_\alpha + 10 Ll c_\lambda - 3(L^2 + l^2)
\end{aligned} \tag{30}
$$

Then, α and λ can be derived as follows:

$$
\begin{aligned}
\alpha &= 2\arctan\left(\frac{-2qlr_1 \mp \sqrt{(2qr_1 l)^2 + 36L^2 l^2 - [r_1^2 + 3(L^2 + l^2) - r_2^2]^2}}{r_1^2 + 3(L^2 + l^2) - r_2^2 + 6Ll} \right) \\
\lambda &= 2\arctan\left(\frac{3l(2r_1 c_\alpha + qL s_\alpha) \mp \sqrt{\begin{matrix} [-3l(2r_1 c_\alpha + qL s_\alpha)]^2 + 81L^2 l^2 \\ -[2r_3^2 - r_2^2 - r_1^2 - 3Ll c_\alpha - 3(L^2 + l^2)]^2 \end{matrix}}}{2r_3^2 - r_2^2 - r_1^2 - 3Ll c_\alpha - 3(L^2 + l^2) - 9Ll} \right)
\end{aligned} \tag{31}
$$

After α and λ are solved from Eqs. (31), Z_o can be solved from Eq. (28) and X_o, Y_o can be solved from Eq. (24).

4.1.2 Velocity and Acceleration Analysis of PS+RPS+SPS PM. Let $\boldsymbol{v}$ and $\boldsymbol{\omega}$ be the linear velocity and angular velocity of moving platform, v_{ri} ($i = 1, 2, 3$) are the velocity along r_i. The inverse velocity of r_i ($i = 1, 2, 3$) can be as follows [5]:

$$
\begin{bmatrix} v_{r1} \\ v_{r2} \\ v_{r3} \end{bmatrix} = \mathbf{J}_\alpha \boldsymbol{V}, \quad \boldsymbol{V} = \begin{bmatrix} \boldsymbol{v} \\ \boldsymbol{\omega} \end{bmatrix}, \quad \mathbf{J}_\alpha = \begin{bmatrix} \boldsymbol{\delta}_1^T & (\boldsymbol{e}_1 \times \boldsymbol{\delta}_1)^T \\ \boldsymbol{\delta}_2^T & (\boldsymbol{e}_2 \times \boldsymbol{\delta}_2)^T \\ \boldsymbol{\delta}_3^T & (\boldsymbol{e}_3 \times \boldsymbol{\delta}_3)^T \end{bmatrix} \tag{32}
$$

here, $\boldsymbol{\delta}_i = \frac{\boldsymbol{a}_i - \boldsymbol{A}_i}{|\boldsymbol{a}_i - \boldsymbol{A}_i|}$, $\boldsymbol{e}_i = \boldsymbol{a}_i - \boldsymbol{o}$.

The workloads can be simplified as a wrench ($\boldsymbol{F}$, $\boldsymbol{T}$) applied onto m at o. Where $\boldsymbol{F}$ is a concentrated force and $\boldsymbol{T}$ is a concentrated torque. ($\boldsymbol{F}$, $\boldsymbol{T}$) are balanced by three active forces $\boldsymbol{F}_{ai}$ ($i = 1$, 2, 3), and three constrained forces $\boldsymbol{F}_{pj}$ ($j = 1, 2, 3$). Each of $\boldsymbol{F}_{ai}$ is applied on and along the active leg r_i. Based on the observe method for finding constrained force/torque [5], we find that the $\boldsymbol{F}_{p1}$ and $\boldsymbol{F}_{p2}$ are exerted on r_1 at a_1. $\boldsymbol{F}_{p3}$ is exerted on r_2 at a_2. From the geometric constraints, the unit vectors $\boldsymbol{f}_j$ of $\boldsymbol{F}_{pj}$ ($j = 1, 2, 3$) are determined as

$$
\boldsymbol{f}_1 = \boldsymbol{f}_3 = \boldsymbol{X} = [1 \quad 0 \quad 0]^T, \quad \boldsymbol{f}_2 = \boldsymbol{Y} = [0 \quad 1 \quad 0]^T \tag{33}
$$

As the constrained forces do no work to the center of the moving platform, we obtain

$$
\begin{aligned}
& F_{pi} \boldsymbol{f}_i \cdot \boldsymbol{v} + (\boldsymbol{e}_i \times F_{pi} \boldsymbol{f}_i) \cdot \boldsymbol{\omega} = 0 \\
& [\boldsymbol{f}_i^T \quad (\boldsymbol{e}_i \times \boldsymbol{f}_i)^T] \boldsymbol{V} = 0
\end{aligned} \tag{34}
$$

The inverse/forward velocities can be derived from Eqs. (32) and (33) as follows:

$$
\boldsymbol{V}_r = \mathbf{J}\boldsymbol{V}, \quad \boldsymbol{V} = \mathbf{J}^{-1}\boldsymbol{V}_r
$$

$$
\mathbf{J} = \begin{bmatrix} \boldsymbol{\delta}_1^T & (\boldsymbol{e}_1 \times \boldsymbol{\delta}_1)^T \\ \boldsymbol{\delta}_2^T & (\boldsymbol{e}_2 \times \boldsymbol{\delta}_1)^T \\ \boldsymbol{\delta}_3^T & (\boldsymbol{e}_3 \times \boldsymbol{\delta}_1)^T \\ \boldsymbol{f}_1^T & (\boldsymbol{e}_1 \times \boldsymbol{f}_1)^T \\ \boldsymbol{f}_2^T & (\boldsymbol{e}_2 \times \boldsymbol{f}_2)^T \\ \boldsymbol{f}_3^T & (\boldsymbol{e}_3 \times \boldsymbol{f}_3)^T \end{bmatrix}, \quad \boldsymbol{V}_r = \begin{bmatrix} v_{r1} \\ v_{r2} \\ v_{r3} \\ 0 \\ 0 \\ 0 \end{bmatrix} \tag{35}
$$

here, $\mathbf{J}$ is a 6×6 Jacobian matrix.

Differentiating both sides of Eq. (34) with respect to time leads to

$$
\begin{aligned} 0 &= [\boldsymbol{f}_i^{\mathrm{T}} \quad (\boldsymbol{e}_i \times \boldsymbol{f}_i)^{\mathrm{T}}]\boldsymbol{A} + [\dot{\boldsymbol{f}}_i^{\mathrm{T}} \quad (\dot{\boldsymbol{e}}_i \times \boldsymbol{f}_i + \boldsymbol{e}_i \times \dot{\boldsymbol{f}}_i)^{\mathrm{T}}]\boldsymbol{V} \\ &= [\boldsymbol{f}_i^{\mathrm{T}} \quad (\boldsymbol{e}_i \times \boldsymbol{f}_i)^{\mathrm{T}}]\boldsymbol{A} + \boldsymbol{V}^T \begin{bmatrix} \mathbf{0}_{3\times3} & \mathbf{0}_{3\times3} \\ \mathbf{0}_{3\times3} & S(\boldsymbol{e}_i)S(\boldsymbol{f}_i) \end{bmatrix}_{6\times6} \boldsymbol{V} \end{aligned} \tag{36}
$$

here

$$
\begin{aligned} &\dot{\boldsymbol{f}}_i^{\mathrm{T}} = \boldsymbol{0}_{3\times1}, \quad \dot{\boldsymbol{e}}_i^{\mathrm{T}} = (\boldsymbol{\omega} \times \boldsymbol{e}_i)^{\mathrm{T}} = [-S(\boldsymbol{e}_i)\boldsymbol{\omega}]^{\mathrm{T}} = \boldsymbol{\omega}^{\mathrm{T}} S(\boldsymbol{e}_i) \\ &\quad (\dot{\boldsymbol{e}}_i \times \boldsymbol{f}_i + \boldsymbol{e}_i \times \dot{\boldsymbol{f}}_i)^{\mathrm{T}} = (\dot{\boldsymbol{e}}_i \times \boldsymbol{f}_i)^{\mathrm{T}} = [-S(\boldsymbol{f}_i)\dot{\boldsymbol{e}}_i]^{\mathrm{T}} \\ &\quad = \dot{\boldsymbol{e}}_i^{\mathrm{T}} S(\boldsymbol{f}_i) = \boldsymbol{\omega}^{\mathrm{T}} S(\boldsymbol{e}_i) S(\boldsymbol{f}_i) \end{aligned}
$$

Based on Eq. (36) and some results in Ref. [5], the acceleration of this PM can be derived as follows:

$$
\begin{aligned} &\boldsymbol{A}_r = \mathbf{J}\boldsymbol{A} + \boldsymbol{V}^T\mathbf{H}\boldsymbol{V}, \quad \boldsymbol{A} = \mathbf{J}^{-1}(\boldsymbol{A}_r - \boldsymbol{V}^T\mathbf{H}\boldsymbol{V}), \\ &\boldsymbol{A}_r = [a_{r1} \quad a_{r2} \quad a_{r3} \quad 0 \quad 0 \quad 0]^T, \\ &\mathbf{H} = [\boldsymbol{h}_1 \quad \boldsymbol{h}_2 \quad \boldsymbol{h}_3 \quad \boldsymbol{h}_4 \quad \boldsymbol{h}_5 \quad \boldsymbol{h}_6], \\ &\boldsymbol{h}_i = \frac{1}{r_i} \begin{bmatrix} -S(\boldsymbol{\delta}_i)^2 & S(\boldsymbol{\delta}_i)^2 S(\boldsymbol{e}_i) \\ -S(\boldsymbol{e}_i)S(\boldsymbol{\delta}_i)^2 & r_i S(\boldsymbol{e}_i)S(\boldsymbol{\delta}_i) + S(\boldsymbol{e}_i)S(\boldsymbol{\delta}_i)^2 S(\boldsymbol{e}_i) \end{bmatrix}_{6\times6}, \\ &\boldsymbol{h}_{i+3} = \begin{bmatrix} \mathbf{0}_{3\times3} & \mathbf{0}_{3\times3} \\ \mathbf{0}_{3\times3} & S(\boldsymbol{e}_i)S(\boldsymbol{F}_i) \end{bmatrix}_{6\times6} \end{aligned} \tag{37}
$$

where a_{ri} $(i=1, 2, 3)$ are the acceleration along r_i. $\mathbf{H}$ is a $6 \times 6 \times 6$ Hessian matrix.

4.1.3 Deformation and Stiffness Analysis of PS + RPS + SPS Parallel Manipulator. Based on virtual work, the formula for solving the statics can be derived as follows:

$$
\boldsymbol{F}_r^T \boldsymbol{V}_r + \begin{bmatrix} \boldsymbol{F} \\ \boldsymbol{T} \end{bmatrix}^T \boldsymbol{V} = 0, \quad \boldsymbol{F}_r = -(\mathbf{J}^{-1})^T \begin{bmatrix} \boldsymbol{F} \\ \boldsymbol{T} \end{bmatrix} \tag{38}
$$

here, $\boldsymbol{F}_r = [F_{a1}\, F_{a2}\, F_{a3}\, F_{p1}\, F_{p2}\, F_{p3}]^T$.

Let δr_i $(i=1, 2, 3)$ denotes the flexibility deformation along $r_i (i=1, 2, 3)$ due to the active force $F_{ai} (i=1, 2, 3)$ lead to

$$
F_{ai} = k_i \delta r_i (1,2,3), \quad k_i = \frac{ES_i}{r_i} \tag{39a}
$$

here, E is the modular of elasticity and S_i is the i-th leg's cross section.

The constrained forces in $r_i (i=1, 2)$ produce flexibility deformation. Let δd_i $(i=1, 2, 3)$ denotes the bending deformation of r_1 due to the constrained forces F_{pi}. The direction of this deformation can be considered along F_{pi}, see Fig. 3.

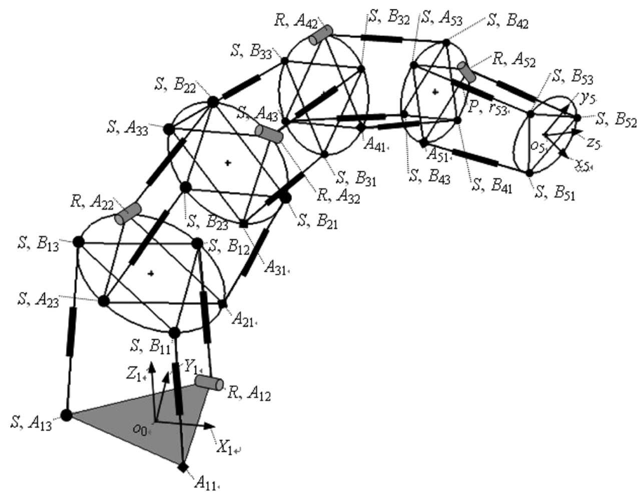

Fig. 2 5(PS + RPS + SPS) S-PM

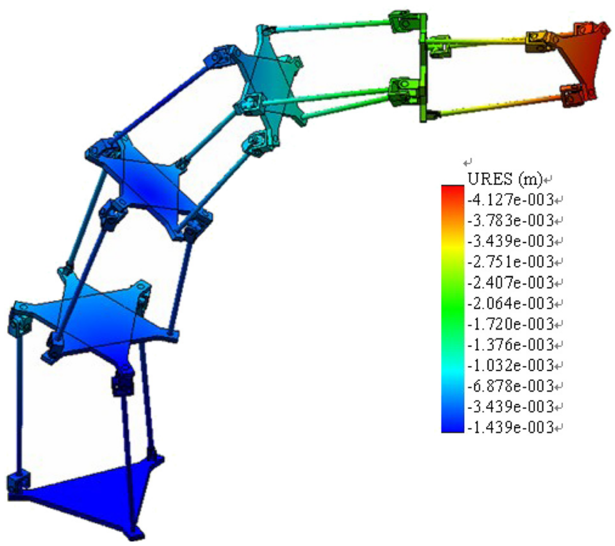

Fig. 3 Solved results of elastic deformations of EF model of 5(PS + RPS + SPS) S-PM

The relation between F_{pi} and δd_i can be expressed as

$$
F_{pi} = s_i \delta d_i (1,2,3), \quad s_i = \frac{3EI}{r_i^3} \tag{39b}
$$

here, I is the moment of inertia.

From Eqs. (39a) and (39b) lead to

$$
\boldsymbol{F}_r = \mathbf{K}_p \begin{bmatrix} \delta \boldsymbol{r} \\ \delta \boldsymbol{d} \end{bmatrix}, \quad \delta \boldsymbol{r} = \begin{bmatrix} \delta r_1 \\ \delta r_2 \\ \delta r_3 \end{bmatrix}, \quad \delta \boldsymbol{d} = \begin{bmatrix} \delta d_1 \\ \delta d_2 \\ \delta d_3 \end{bmatrix},
$$

$$
\mathbf{K}_p = \begin{bmatrix} k_1 & 0 & 0 & 0 & 0 & 0 \\ 0 & k_2 & 0 & 0 & 0 & 0 \\ 0 & 0 & k_3 & 0 & 0 & 0 \\ 0 & 0 & 0 & s_1 & 0 & 0 \\ 0 & 0 & 0 & 0 & s_2 & 0 \\ 0 & 0 & 0 & 0 & 0 & s_3 \end{bmatrix} \tag{40}
$$

Table 1 The length, velocity, and acceleration of r_i for single PS + RPS + SPS PM

	r_1 (m)	r_2 (m)	r_3 (m)	v_{r1} (m/s)	v_{r2} (m/s)	v_{r3} (m/s)	a_{r1} (m/s^2)	a_{r2} (m/s^2)	a_{r3} (m/s^2)
PM 1	1.20	1.40	1.50	0.2	0.2	0.2	0.1	0.1	0.1
PM 2	1.10	1.30	1.40	0.2	0.2	0.2	0.1	0.1	0.1
PM 3	1.00	1.20	1.30	0.2	0.2	0.2	0.1	0.1	0.1
PM 4	0.90	1.10	1.20	0.2	0.2	0.2	0.1	0.1	0.1
PM 5	0.80	1.00	1.10	0.2	0.2	0.2	0.1	0.1	0.1

here $\delta r_i (i=1, 2, 3)$ denotes the flexibility deformation produced by active force $F_{ai} (i=1, 2, 3)$ and $\delta d_i (i=1, 2, 3)$ denotes the bending deformation produced by constrained forces $F_{pi} (i=1, 2, 3)$.

Let $\delta \boldsymbol{x} = [\delta x \; \delta y \; \delta z]^T$, $\delta \boldsymbol{\theta} = [\delta\theta_x \; \delta\theta_y \; \delta\theta_z]^T$ denote the linear and angle deformations of moving platform. From the principle of virtue work leads to

$$\boldsymbol{F}_r^T \begin{bmatrix} \delta \boldsymbol{r} \\ \delta \boldsymbol{d} \end{bmatrix} + \begin{bmatrix} \boldsymbol{F} \\ \boldsymbol{T} \end{bmatrix}^T \begin{bmatrix} \delta \boldsymbol{x} \\ \delta \boldsymbol{\theta} \end{bmatrix} = 0 \tag{41}$$

From Eqs. (38), (40), and (41) lead to

$$\begin{aligned} \begin{bmatrix} \delta \boldsymbol{x} \\ \delta \boldsymbol{\theta} \end{bmatrix} &= \mathbf{J} \begin{bmatrix} \delta \boldsymbol{r} \\ \delta \boldsymbol{d} \end{bmatrix}, \quad \begin{bmatrix} \boldsymbol{F} \\ \boldsymbol{T} \end{bmatrix} = \mathbf{K} \begin{bmatrix} \delta \boldsymbol{x} \\ \delta \boldsymbol{\theta} \end{bmatrix}, \\ \begin{bmatrix} \delta \boldsymbol{x} \\ \delta \boldsymbol{\theta} \end{bmatrix} &= \mathbf{K}^{-1} \begin{bmatrix} \boldsymbol{F} \\ \boldsymbol{T} \end{bmatrix}, \quad \mathbf{K} = -\mathbf{J}^T \boldsymbol{K}_p \mathbf{J} \end{aligned} \tag{42}$$

$\mathbf{K} = -\mathbf{J}^T \mathbf{K}_p \mathbf{J}$ is the stiffness matrix considering both active forces and constrained forces.

4.2 Analysis of *k*(PS + RPS + SPS) S-PM. The k(PS + RPS + SPS) S-PM is formed by k PS + RPS + SPS PMs connected in series. The lower platform of PM i $(i=2,\ldots, k)$ can be obtained by the upper platform of PM i-1 anticlockwise rotate with the its perpendicular by $60 \times (-1)^i$ deg.

Let A_{ij} and B_{ij} $(i=1, 2,\ldots, k; j=1, 2, 3)$ denote three vertices of the lower platform and upper platform of PM i, respectively. Let r_{i1}, r_{i2}, and r_{i3} $(i=1, 2,\ldots,k)$ denote the PS, RPS, and SPS leg and their length, respectively, in PM i. Let L_i be the distance from the center of lower platform to A_{ij}. Let l_i be the distance from the center of upper platform to B_{ij}.

Let $\{n_{i0}\}$ be a coordinate $o_{i\text{-}1}\text{-}X_iY_iZ_i$ $(i=1, 2,\ldots, k)$ fixed on the center of lower platform of PM i with some conditions $(X_i \perp A_{i1}A_{i2},\ Y \| A_{i1}A_{i2},\ Z \perp X_i,\ Z \perp Y_i)$ for its coordinate axes are satisfied. Here, o_0 is the center of base. Let $\{n_{i1}\}$ be a coordinate $o_i\text{-}x_iyz_i$ fixed on the center of upper platform of PM i with some conditions $(x_i \perp B_{i1}B_{i2},\ y \| B_{i1}B_{i2},\ z \perp x_i,\ z \perp y_i)$ for its coordinate axes are satisfied.

When r_{i1}, r_{i2}, and r_{i3} $(i=1, 2,\ldots,k)$ are given, ${}^{n_{i0}}\boldsymbol{o}_i$ can be solved from Eqs. (31) and (24). ${}^{n_{i0}}_{n_{i1}}\mathbf{R}$ can be solved from Eqs. (31) and (23). Then, ${}^{n_{10}}_{n_{i0}}\mathbf{R}$ and ${}^{n_0}\boldsymbol{o}_k$ can be solved from Eq. (1), where

$${}^{(i-1)1}_{n_{i0}}\mathrm{R} = \begin{bmatrix} \cos[60\text{ deg} \times (-1)^i] & -\sin[60\text{ deg} \times (-1)^i] & 0 \\ \sin[60\text{ deg} \times (-1)^i] & \cos[60\text{ deg} \times (-1)^i] & 0 \\ 0 & 0 & 1 \end{bmatrix}$$

Let v_{rij} and a_{rij} be the velocity and acceleration of r_{ij}, respectively. When given v_{rij} $(i=1, 2, \ldots, k;\ j=1, 2, 3)$, ${}^{n_{i0}}\boldsymbol{v}_{oi}$, ${}^{n_{i0}}_{n_{i1}}\boldsymbol{\omega}$, ${}^{n_{i0}}\boldsymbol{a}_{oi}$, ${}^{n_{i0}}_{n_{i1}}\boldsymbol{\varepsilon}$ can be solved from Eqs. (35) and (37). Then, ${}^{n_{10}}_{n_{k1}}\boldsymbol{\omega}$ and ${}^{n_{10}}\boldsymbol{V}_{ok}$ can be solved from Eqs. (3) and (4), ${}^{n_{10}}_{n_{k1}}\boldsymbol{\varepsilon}$ and ${}^{n_{10}}\boldsymbol{a}_{ok}$ can be solved from Eqs. (5) and (7).

From Eqs. (35) and (8*b*), $\mathbf{J}_{si}$ and $\mathbf{J}_{Ri}$ can be solved. When given ${}^{n_0}\boldsymbol{F}_o$ and ${}^{n_0}\boldsymbol{T}_o$, the statics can be solved form Eq. (11).

Let δr_{ij} $(i=1, 2, \ldots, k;\ j=1, 2, 3)$ and δd_{ij} be the flexibility and bending deformations of PM i, the deformations can be solved from Eqs. (39*a*) and (39*b*), the stiffness matrix $\mathbf{K}_i$ and the deformation $\delta \boldsymbol{\rho}_i$ of upper platform of PM i can be solved from Eq. (42).Then, the deformation $\delta \boldsymbol{\rho}$ of the terminal platform and the stiffness matrix of this S-PM can be solved Eqs. (14) and (15), respectively.

Table 2 The pose of single PS + RPS + SPS PM

	α (deg)	λ (deg)	X_o (m)	Y_o (m)	Z_o (m)
PM 1	12.496	−126.66	0.4438	−0.01557	1.0939
	12.496	14.832	0.037524	−0.0751	1.3623
	−112.88	−37.821	0.083446	−0.8218	0.8474
	−112.88	131.74	0.46163	−0.4964	0.7100
PM 2	14.04	−129.7	0.40732	−0.0188	1.0247
	14.04	16.756	0.038673	−0.0781	1.2616
	−115.46	−39.438	0.081448	−0.7544	0.8019
	−115.46	136.32	0.42683	−0.4780	0.6703
PM 3	16.025	−133.5	0.37004	−0.0231	0.9557
	16.025	19.272	0.040191	−0.0820	1.1607
	−118.71	−41.538	0.079686	−0.6857	0.7574
	−118.71	141.91	0.38998	−0.4588	0.6331
PM 4	18.673	−138.43	0.33165	−0.0290	0.8872
	18.673	22.718	0.042306	−0.0872	1.0594
	−122.92	−44.398	0.078318	−0.6148	0.7140
	−122.92	148.9	0.35038	−0.4380	0.5996
PM 5	22.392	−145.12	0.29162	−0.0374	0.8190
	22.392	27.764	0.045484	−0.0945	0.9574
	−128.65	−48.561	0.07768	−0.5407	0.6724
	−128.65	157.97	0.307	−0.4139	0.5709

Table 3 The position, velocity, and acceleration of terminal platform of 5(PS + RPS + SPS) S-PM

${}^{\{n0\}}o_k$ (m)	${}^{\{n0\}}v_k$ (m/s)	${}^{\{n0\}}\omega_k$ (deg/s)	${}^{\{n0\}}a_k$ (m/s^2)	${}^{\{n0\}}\varepsilon_k$ (deg/s^2)
3.0208	0.53502	0.25454	0.2669	0.0422
−0.7363	−0.08853	0.83891	−0.0432	0.1599
4.0243	0.68036	0.15453	0.3385	0.0556

Table 4 Active force and constrained force of single PS + RPS + SPS PM

	F_{a1} (N)	F_{a2} (N)	F_{a3} (N)	F_{r1} (N)	F_{r2} (N)	F_{r3} (N)
PM 1	192.04	−29.151	−103.54	15.264	20.307	12.507
PM 2	162.27	−105.78	−1.5083	11.063	5.739	28.67
PM 3	95.23	87.201	−123.75	−45.554	32.767	43.748
PM 4	132.92	54.616	−148.57	7.8862	39.738	36.908
PM 5	−181.23	224.2	−9.1093	−4.5507	75.215	−36.853

5 Example

A 5(PS + RPS + SPS) S-PM in Fig. 2 is formed by 5 PS + RPS + SPS PMs connected in series. Set $L_i = 1 - 0.1 \times (i-1)$, $l_i = 0.9 - 0.1 \times (i-1)$. $E = 2.11 \times 10^{11}$ Pa, $EI = 26{,}502$ N m^2, $S_i = 0.0013$ m^2. $G = 80 \times 10^9$ Pa, $I_p = 2.5120 \times 10^{-7}$ m^4. The length,

Table 5 Deformations in the legs for single PS + RPS + SPS PM (10^{-4} m)

	δr_1	δr_2	δr_3	δd_1	δd_2	δd_3
PM 1	0.0086956	−0.0015399	−0.0058604	3.3175	4.4136	4.3165
PM 2	0.0067353	−0.005189	−0.0000797	1.8521	0.96077	7.9226
PM 3	0.0035934	0.0039485	−0.0060703	−5.7297	4.1214	9.5084
PM 4	0.004514	0.002267	−0.0067272	0.7231	3.6437	6.1787
PM 5	−0.0054707	0.0084599	−0.0003781	−0.29306	4.8438	−4.6353

velocity, and acceleration of r_i for PM i ($i = 1,2,\ldots,5$) are given in Table 1.

The poses of PM i ($i = 1, 2, \ldots, 5$) are solved from Eqs. (24), (28), and (31), see Table 2. The results show that the single PS + RPS + SPS PM have four solutions. By using CAD software, the simulation mechanism can be created [13], and the forward kinematic can also be solved by the simulation mechanism. From the results of the simulation and the analytic methods, it can be seen that the simulation solution is identical with the analytic solution. The second solution is selected for subsequent calculation, see Table 2.

Table 6 The simulated result based on finite element model and the calculated result based on stiffness model for the deformation of *m*

Elastic deformation of o (mm)		
	FE model	Analytics
δx	−0.0563	−0.0669
δy	−2.225	−2.5736
δz	−0.0141	−0.0101

The position, velocity, and acceleration of terminal platform of 5(PS + RPS + SPS) S-PM are solved from Eqs. (3)–(5) and (7), see Table 3. When given the workloads applied at o_k ${}^{no}\boldsymbol{F}_o = [-20\ -30\ -60]^T$ N, ${}^{no}\boldsymbol{T}_o = [-30\ -30\ 100]^T$ N·m, the active forces and constrained forces of r_i for PM i can be solved from Eq. (38), see Table 4. The deformations of r_i for PM i can be solved from Eqs. (39*a*) and (39*b*), see Table 5.

The deformation of the terminal platform of 5(PS + RPS + SPS) S-PM is derived from Eq. (14) as

$$\delta\boldsymbol{\rho} = 10^{-3}[-0.0669\ \ -2.5736\ \ -0.0101\ \ -1.2025\ \ 0.9403\ \ -3.0546]^T$$

The stiffness matrix of 5(PS + RPS + SPS) S-PM is derived from Eq. (15) as follows:

$$\mathbf{K} = 10^5\begin{bmatrix} -0.57209 & 0.12852 & -0.085354 & -0.036468 & -0.56074 & -0.18826 \\ 0.12852 & -0.15185 & -0.0023684 & -0.053095 & 0.34759 & 0.35124 \\ -0.08535 & -0.002368 & -0.7545 & -0.009258 & 0.071977 & 0.22857 \\ -0.03647 & -0.053095 & -0.0092575 & -0.14603 & -0.1821 & 0.14521 \\ -0.56074 & 0.34759 & 0.071977 & -0.1821 & -3.0485 & -1.0493 \\ -0.18826 & 0.35124 & 0.22857 & 0.14521 & -1.0493 & -1.0001 \end{bmatrix}$$

To verify the stiffness model, A 3D assembly mechanism and a finite element (FE) model of 5(PS + RPS + SPS) S-PM is generated in SoldWork7/Simulation according to relative geometry and material parameters described above. In the FE model, the spherical joint is replaced by three revolute joints. The linear active leg with prismatic joint is formed using the elastic linear rod. A fixed constraint is added onto base. The simulated result based on finite element model for the deformation of m is solved as shown in Fig. 3 and Table 6.

It is well known that the solved results of FE model are related to finite element dimension and type, solver, reasonable boundary constraints, and connection constraints. Therefore, in most cases, the solved results of FM model are approximate of analytical solutions. From the calculated results and simulated values, it is known that established stiffness model are basically coincident with that of the FE model, which is acceptable for stiffness analysis.

6 Conclusions

The statics and stiffness model of S-PMs formed by k PMs connected in series is established. This model is based on the analytical result of single PM. To illustrate this model, a novel k(PS + RPS + SPS) S-PM is analyzed.

The kinematics of single PS + RPS + SPS PM is solved in closed form. It is shown that the forward kinematics of the PS + RPS + SPS manipulator has apparent analytical form and has four solutions. The stiffness of the PS + RPS + SPS PM is analyzed by taking into account the deformation produced both by active forces and constrained forces, and the 6×6 stiffness matrix is derived subsequently. On analyzing the single PS + RPS + SPS PM, the kinematics, statics, and stiffness of k(PS + RPS + SPS) S-PM are solved. The analytic results are verified by its simulation mechanism.

Acknowledgment

The authors would like to acknowledge Project (51175447) supported by the National Natural Sciences Foundation of China (NSFC),the Key planned project of Hebei application foundation (11962127D) and the research and development project of science and technology of Qinhuangdao city (201101A140).

Nomenclature

${}^{n_{jb}}\boldsymbol{o}_i$ = the position vectors of the center of PM i relative to $\{n_{jb}\}$ ($j = 1, \ldots, k$; $b = 0, 1$)

${}^{n_{i0}}\boldsymbol{o}_i$, ${}^{n_{10}}\boldsymbol{o}_i$ = the position vectors for the center of upper platform of PM i relative to $\{n_{i0}\}$ and $\{n_{10}\}$

${}^{n_{jb}}_{n_{sc}}\mathbf{R}$ = the rotational matrixes of $\{n_{sc}\}$ ($s = 1,\ldots, k$; $c = 0, 1$) relative to $\{n_{jb}\}$

${}^{n_{i0}}_{n_{i1}}\mathbf{R}$ = the rotational matrix from upper platform to lower platform for PM i

${}^{n_{10}}_{n_{i1}}\mathbf{R}$ = the rotational matrix from terminal platform to base

${}^{n_{jb}}\boldsymbol{v}_{oi}$, ${}^{n_{jb}}\boldsymbol{a}_{oi}$ = the linear velocity and acceleration of the upper platform of PM i relative to $\{n_{jb}\}$

${}^{n_{jb}}_{n_{sc}}\boldsymbol{\omega}$, ${}^{n_{jb}}_{n_{sc}}\boldsymbol{\varepsilon}$ = the angular velocity and acceleration of $\{n_{sc}\}$ relative to $\{n_{jb}\}$

${}^{n_{i0}}\boldsymbol{v}_{oi}$, ${}^{n_{i0}}_{n_{i1}}\boldsymbol{\omega}$, ${}^{n_{i0}}\boldsymbol{a}_{oi}$, ${}^{n_{i0}}_{n_{i1}}\boldsymbol{\varepsilon}$ = the linear velocity, angular velocity, linear acceleration, and angular acceleration of upper platform relative to lower platform of PM i

${}^{n_{10}}\boldsymbol{v}_{ok}$, ${}^{n_{10}}_{n_{k1}}\boldsymbol{\omega}$, ${}^{n_{10}}_{n_{k0}}\boldsymbol{\varepsilon}$, ${}^{n_{10}}_{n_k}\boldsymbol{a}_{ok}$ = the linear velocity, angular velocity, linear acceleration, and angular acceleration of terminal platform relative to base coordinate n_{10}

$\boldsymbol{F}_o$, $\boldsymbol{T}_o$ = the external force and torque applied on terminal platform

$\boldsymbol{F}_{si}$ = the six dimensional vector formed by active and constrained forces/torques

$\boldsymbol{V}_{si}$ = the six dimensional vector formed by actuator velocities and 0 elements

$\mathbf{J}_{si}$ = the inverse Jacobian matrix of PM i

$\delta\boldsymbol{\rho}_i$, $\delta\boldsymbol{\rho}$ = the vectors of deformation associate with the moving platform of PM i and the whole S-PM

$\mathbf{K}_i$, $\mathbf{K}$ = the stiffness matrix of PM i and the whole S-PM

${}^{n_0}\boldsymbol{F}_o$, ${}^{n_0}\boldsymbol{T}_o$ = the workloads $\boldsymbol{F}_o$ and $\boldsymbol{T}_o$ expressed in $\{n_0\}$

${}^{n_i}\boldsymbol{F}_{oi}$, ${}^{n_i}\boldsymbol{T}_{oi}$ = the concentrative force and torque at the upper platform for PM i expressed in $\{n_i\}$

References

[1] Angeles, J., 2003, *Fundamentals of Robotic Mechanical Systems*, Springer-Verlag, Berlin.

[2] Merlet, J. P., 2000, *Parallel Robots*, Kluwer Academic Publishers, London.

[3] Gallardo, J., and Camarillo, K. A., 2011, "Inverse Jerk Analysis of Symmetric Zero-Torsion Parallel Manipulators," Rob. Auton. Syst., **59**(11), pp. 859–866.

[4] Hong, M. B., and Choi, Y. J., 2011, "Formulation of Unique Form of Screw Based Jacobian for Lower Mobility Parallel Manipulators," ASME J. Mech. Rob., **3**(1), p. 011002.

[5] Lu, Y., and Hu, B., 2008, "Unification and Simplification of Velocity/Acceleration of Limited-Dof Parallel Manipulators With Linear Active Legs," Mech. Mach. Theory, **43**(9), pp. 1112–1128.

[6] Merlet, J. P., 1989, "Singular Configurations of Parallel Manipulators and Grassman Geometry," Int. J. Rob. Res., **8**(5), pp. 45–56.

[7] Zhang, D., 2005, "On Stiffness Improvement of the Tricept Machine Tool," Robotica, **23**(3), pp. 377–386.

[8] Staicu, S., 2011, "Dynamics of the 6-6 Stewart Parallel Manipulator," Rob. Comput.-Integr. Manufact., **27**(1), pp. 212–220.

[9] Zhao, Y., and Gao, F., 2009, "Inverse Dynamics of the 6-dof Out-Parallel Manipulator by Means of the Principle of Virtual Work," Robotica, **27**(2), pp. 259–268.

[10] Romdhane, L., 1999, "Design and Analysis of a Hybrid Serial-Parallel Manipulator," Mech. Mach. Theory, **34**, pp. 1037–1055.

[11] Tanev, T., 2000, "Kinematics of a Hybrid (Parallel-Serial) Robot Manipulator," Mech. Mach. Theory, **35**, pp. 1183–1196.

[12] Zheng, X. Z., Bin, H. Z., and Luo, Y. G., 2004, "Kinematic Analysis of a Hybrid Serial-Parallel Manipulator," Int. J. Adv. Manuf. Technol., **23**(11–12), pp. 925–930.

[13] Lu, Y., and Hu, B., 2006, "Solving Driving Forces of 2(3-SPR) Serial-Parallel Manipulator by CAD Variation Geometry Approach," Trans. ASME J. Mech. Des., **128**(6), pp. 1349–1351.

[14] Lu, Y., Hu, B., and Sun, T., 2009, "Analyses of Velocity, Acceleration, Statics, and Workspace of a 2(3-SPR) Serial-Parallel Manipulator," Robotica, **27**(4), pp. 529–538.

[15] Lu, Y., and Hu, B., 2009, "Solving Active Wrench of Limited-dof Parallel Manipulators Based on Translational/Rotational Jacobina Matrices," Proc. IMechE Part K: J. Multi-body Dyn., **223**(8), pp. 221–229.

[16] Gallardoa, J., Orozcoa, H., Rico, J. M., and González-Galván, E. J., 2009, "A New Spatial Hyper-Redundant Manipulator," Rob. Comput.-Integr. Manufact., **25**(4–5), pp. 703–708.

[17] Gallardo, J., Lesso, R., Rico, J., and Alici, G., 2011, "The Kinematics of Modular Spatial Hyper-Redundant Manipulators Formed From RPS-Type Limbs," Rob. Auton. Syst., **59**(1), pp. 12–21.

[18] Ibrahim, O., and Khalil, W., 2010, "Inverse and Direct Dynamic Models of Hybrid Robots," Mech. Mach. Theory, **45**(4), pp. 627–640.

[19] Shugen, M., and Naoki, T., 2006, "Analysis of Creeping Locomotion of a Snake-Like Robot on a Slope," Auton. Rob., **20**(1), pp. 15–23.

[20] Hanan, M. W., and Walker, I. A., 2003, "Kinematics and the Implementation of an Elephant's Trunk Manipulator and Other Continuum Style Robots," J. Rob. Syst., **20**(2), pp. 45–63.

[21] Moosavian, S., and Pourreza, A., 2010, "Heavy Object Manipulation by a Hybrid Serial-Parallel Mobile Robot," Int. J. Rob. Autom., **25**(2), pp. 109–120.

[22] Liang, C., Ceccarelli, M., and Carbone, G., 2011, "Experimental Characterization of Operation of a Waist-Trunk System With Parallel Manipulators," Chin. J. Mech. Eng., **24**(5), pp. 713–722.